

Automated Selection and Placement of Single Cells Using Vision-Based Feedback Control

Yasser H. Anis, *Member, IEEE*, Mark R. Holl, *Member, IEEE*, and Deirdre R. Meldrum, *Fellow, IEEE*

Abstract—We present a robotic manipulation system for automated selection and transfer of individual living cells to analysis locations. We begin with a commonly used cell transfer technique using glass capillary micropipettes to aspirate and release living cells suspended in liquid growth media. Using vision-based feedback and closed-loop process control, two individual three-axis robotic stages position the micropipette tip in proximity to the cell of interest. The cell is aspirated and the tip is moved to a target location where the cell is dispensed. Computer vision is used to monitor and inspect the success of the dispensing process. In our initial application, the target cell destination is a microwell etched in a fused silica substrate. The system offers a robust and flexible technology for cell selection and manipulation. Applications for this technology include embryonic stem cells transfer, blastomere biopsy, cell patterning, and cell surgery.

Note to Practitioners—The need to apply advanced automation methods to sample preparation and analysis in the life sciences has increased at a steady pace. One field of research requiring extreme fidelity for sample preparation is the analysis of cell physiology with resolution down to the single cell. Key features of such systems are the ability to identify cells of interest, select them, and place them at predetermined points in space and time for analysis in configurations where cells are observed while they respond to some external stimulus. We present an automated cell manipulation system using capillary micropipettes and vision-guided robotics. This system implements automation of cell selection, micropipette positioning, cell placement, and release. The system has the ability to transfer living, individual cells from a culture dish to target locations with a 100% success rate. Our incorporation of a fluidic manipulator for aspirating and dispensing picoliter-volumes of fluid with precise flow rate control will enable knowledge of the exact location of an aspirated cell within the micropipette, reducing cell loss and increasing cell transfer yields and rates. The proposed robotic system provides essential functionality with single-cell resolution and is therefore the appropriate technology for practitioners with this functional need.

Manuscript received March 24, 2009; revised July 31, 2009. This paper was recommended for publication by Associate Editor Y. Sun and Editor V. Kumar upon evaluation of the reviewers' comments. This work was supported in part by the National Institutes of Health NHGRI Centers of Excellence in Genomic Science (Grant 5 P50 HG002360, D. Meldrum (PI) and M. Lidstrom).

Y. Anis and M. Holl are with the Center for Ecogenomics, The Biodesign Institute, Arizona State University, Tempe, AZ 85287 USA (e-mail: yasser.anis@asu.edu, mark.holl@asu.edu).

D. Meldrum is with the Ira A. Fulton School of Engineering, and the Center for Ecogenomics, The Biodesign Institute, Arizona State University, Tempe, AZ 85287 USA (e-mail: deirdre.meldrum@asu.edu).

Color versions of one or more of the figures in this paper are available online at <http://ieeexplore.ieee.org>.

This paper has supplementary downloadable material available at <http://ieeexplore.ieee.org>, provided by the authors. This includes one multimedia AVI format movie clip, which shows the automated selection and placement of a single cell to a microwell using vision-based feedback control. This material is 12 MB in size.

Digital Object Identifier 10.1109/TASE.2009.2035709

Index Terms—Automation, cell manipulation, closed-loop control, feature recognition, image processing, visual servoing.

I. INTRODUCTION

THE oldest and most commonly used approach for single-cell manipulation uses glass capillary micropipettes [1]. A negative pressure applied to growth media filled capillary, immersed in a cell culture dish, controls the aspiration of a desired cell. A positive pressure dispenses the cell. In several studies, micropipette aspiration of cells was used to quantify the mechanical properties of cells, and the forces between cells and surfaces [2], [3]. Motion stages with multiple degrees-of-freedom were used to manually manipulate the micropipette and accurately control its tip position to perform either micromanipulation or microinjection. Commercially available manual cell manipulation systems include the Quixell (Stoelting, Wood Dale, IL) and TransferMan NK 2 (Eppendorf, Hamburg, Germany) systems. The Quixell system provides some degree of automation through the ability to have programmed destination locations within microwells on a microplate. Its cell selection and collection processes are performed manually using a keypad and a joystick [4]. Such single-cell manipulations, using a micropipette, have been demonstrated to be reliable, minimally traumatic, and widely accepted. However, in the absence of cell selection and placement automation, it is time consuming, labor intensive, and unsuitable for processing large numbers of single cells.

Other approaches for single-cell manipulation have been advanced. Ashkin [5] proposed using electromagnetic field forces, exerted by a strongly focused laser, to trap and move cells. The development of these “optical tweezers” led to clinical applications in such areas as *in vitro* fertilization, and manipulation of suspensions of red blood cells [7], [6]. Trapping configurations have been demonstrated with high-energy infrared (IR) light. IR light is capable of producing large forces, innocuous to cells, but collateral thermal stress may ensue [5]. Electrical forces have also been used for microscale cell manipulations either by electrophoresis (EP) or dielectrophoresis (DEP). Classification as EP or DEP depends on whether the forces act upon the fixed or induced charge of a particle. Both have been successfully used for cell sorting [8]. As with optical tweezers, all cell manipulations take place in solution.

Despite the sophistication of these alternative methods, capillary-based cell manipulation using aspiration and dispensing remains the most widely accepted and used technique. In this work, we address a fundamental need in the area of biological laboratory automation: fully automated cell manipulation using

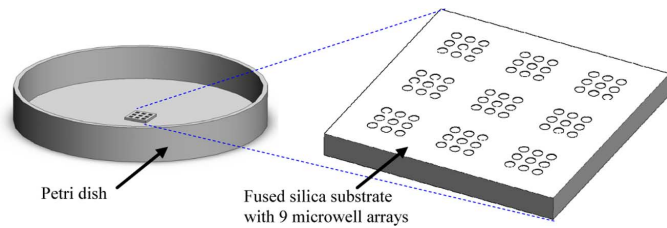


Fig. 1. Schematic of a fused silica substrate, fixed to the bottom of a petri dish. The substrate includes nine microwell arrays, each consisting of nine microwells.

capillary micropipettes and associated robotics. This system implements full automation of cell selection, micropipette positioning, cell placement, and release. This comparatively inexpensive, robust, and flexible technology can be deployed in biology laboratories with creative adaptations, enabling new experimental protocols. Other than the manipulation of suspension cells, the system can be used for applications such as the transfer of embryonic stem cells (ES), or blastomere biopsies during preimplantation genetic diagnosis (PGD).

We first applied the system in a project with the aim to address questions surrounding biological cellular heterogeneity. In order to realize the promise of genomics in curing major diseases, it is necessary to develop precise tools for multiparameter analysis of single cells, and apply these tools to the understanding of biological questions involving the heterogeneity of cell populations. In the Microscale Life Sciences Center (MLSC) [9], we are developing a high-throughput, multiparameter integrated system to monitor in parallel cellular parameters such as respiration rates and gene expression [10]–[12].

The objective of this research was to develop the capability to automatically select and pick up a single cell from a culture dish, manipulate and move the cell to a specified target location, and release the cell. Target locations could be microplate wells or PCR tube caps. In this work, target locations are microwells etched in a fused silica substrate [13], fixed to the bottom of a petri dish, as shown in Fig. 1. The microwells are arranged in 3×3 arrays of nine microwells. The loading process involves a repeated selection and placement of one live cell into each microwell. When completely loaded with single cells, the microwells arrays are incubated and then used for single-cell analyses. In principle, the system can manipulate any type of cell suspended in solution, including mammalian cells, macrophages, and bacteria cells. Preliminary results of this work were reported in Anis *et al.* [14].

II. SYSTEM DESCRIPTION AND APPARATUS

A six-axis cell manipulation robotic system was built, shown in Fig. 2. The system is constructed of three subsystems: a motion control system, a vision system, and a fluid control system. The three subsystems are integrated to enable both manual and automated cell manipulation through the use of software. The motion control system consists of two sets of three-degree-of-freedom (DOF) translation stages, an X_t - Y_t - Z_t stage, and an X - Y - Z stage, assembled on an inverted microscope. The cell

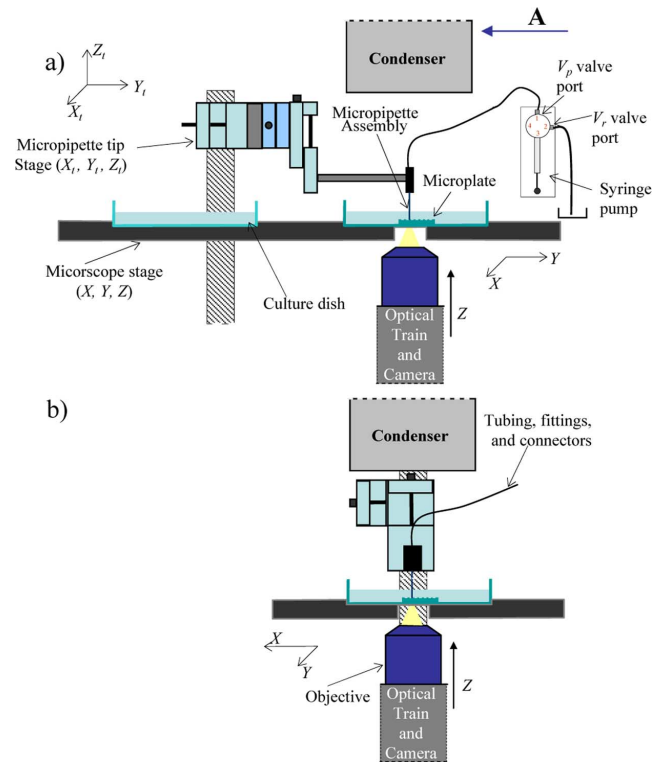


Fig. 2. Schematic of the six-axis robotic workstation. (a) Front view, showing main hardware components. (b) Side view, as seen from the direction “A” displayed in (a).

selection and placement are monitored using vision-based feedback, captured using a microscope and a charge-coupled device (CCD) camera. A glass capillary micropipette is used as the robot end effector. Single cells suspended in cell growth media in a culture dish are aspirated, moved, and dispensed into target microwells. Applying negative or positive pressures to the medium-filled micropipette controls the cell aspiration and dispensing.

A. Motion Control System

The micropipette tip positioning stage X_t - Y_t - Z_t (T-LS28-I, Zaber, Richmond, BC, Canada) and the microscope positioning stage X - Y - Z (MS-2000, ASI, Eugene, OR) comprise the motion control system stages. The X_t - Y_t - Z_t stage manipulates the micropipette in space for single-cell pick and place operations. The X_t - Y_t stage uses DC servomotors to displace the micropipette in the x_t - and y_t -directions to vertically align the micropipette tip with the center of the microscope field of view. The Z_t stage controls the micropipette vertical displacement (in the z_t -direction). The X_t - Y_t - Z_t stage is controlled through serial connection to a computer. The petri culture dish is mounted to a 2-axis X - Y microscope motorized stage that also carries a microwell array substrate, bonded to the bottom of another petri dish. The X - Y stage displaces the culture dish and the microwell array substrate in the x - and y -directions. The position of the X - Y stage depends on whether a cell is being aspirated from the culture dish or dispensed into a microwell. The Z stage vertically moves the microscope objective in the z -direction, to bring monitored objects into focus. The

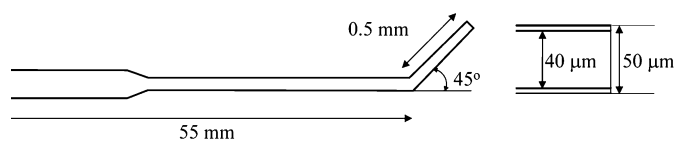


Fig. 3. Schematic of the micropipette capillary showing dimensions.

X - Y - Z stage is controlled either manually using a joystick or algorithmically through a serial connection.

B. Vision System

The vision system includes an inverted microscope (TE-2000U, Nikon, Tokyo, Japan) with a 10 \times objective (CFI Plan Achromat, Nikon) having a numerical aperture of 0.25, and a working distance of 10.5 mm. Brightfield illumination is supplied by a 100 W halogen light source (LHS-H100P-1, Nikon) with a 12 V power supply. A 5 megapixel (2560 \times 1920 pixels) FireWire™ CCD color camera (Micropublisher 5.0, QImaging, Surrey, BC, Canada) is used to capture images.

C. Fluid Control System

The fluid control subsystem consists of a syringe pump, a micropipette, and tubings and fittings. The syringe pump (Versa 6, Kloehn, Las Vegas, NV) incorporates a 10 μ L glass syringe. The flow rate can be controlled between 0.01 and 2 μ L/s, achieving a volume resolution of 200 pL. The piston displacement and velocity are directly proportional to the volume and rate of flow. The pump is connected to a micropipette through poly-etheretherketone (PEEK) tubing, fittings, and connectors (Upchurch Scientific, Oak Harbor, WA). The pump has a single four-port rotary distribution valve, of which two distribution ports are used. One port (V_p) is connected to the micropipette tubing and the other (V_r) is connected to a reservoir. We used commercially available borosilicate glass micropipettes (MBB-FP-L-45, Humagen, Charlottesville, VA) with 40 μ m inner diameter (ID), 50 μ m outer diameter (OD), where the tip (0.5 mm long) is angled at 45 $^\circ$, as shown in Fig. 3. The 40 μ m ID micropipettes are suitable to manipulate suspended cells of 5 to 35 μ m diameters. The micropipette tip was chosen to have an inclination angle of 45 $^\circ$ to the horizontal to provide an unobstructed view of the cell before and during aspiration. The micropipette is connected to the X_t - Y_t - Z_t stage through a holding fitting. The micropipette, assembled to the holding fitting is called the micropipette assembly, shown in Fig. 2.

D. Software

We developed control software, using LabVIEW (v8.5, National Instruments, Austin, TX). An Intel Core 2 Duo processor personal computer was used, running at 2.13 GHz with 3.0 GB memory. The graphical user interface (GUI), shown in Fig. 4, enables manual, semi-automated, or automated control of the different stages of the cell manipulation process. The software consists of four modules working in parallel, controlling the positioning of the micropipette stages, the positioning of the microscope stages, the syringe pump, and the vision system. Operation of the two positioning stage modules includes control of the absolute position and velocity of the stage motors. The position of each stage motor is used as feedback for the closed-loop control of the system. The pump software module controls the

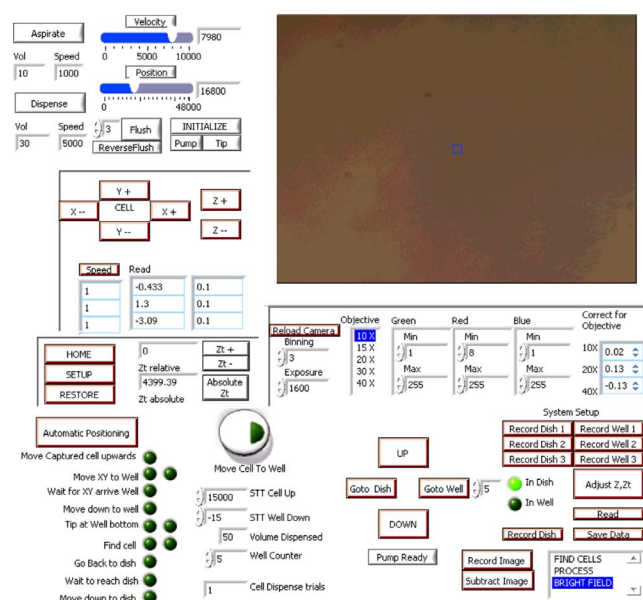


Fig. 4. Labview-based GUI control software that enables both manual and automated control of the cell pickup and placement processes.

displacement, velocity, and acceleration of the syringe piston in addition to the valve position settings between distribution valve ports V_p and V_r . The vision module controls the camera settings, image acquisition, image processing, and object recognition. Camera settings include binning, exposure, and image type, whether colored (RGB) or grayscale. Image processing controls include brightness, contrast, gamma correction, and settings of upper and lower thresholds. Object recognition controls include the specification of maximum and minimum object sizes, aspect ratio, and search area. The vision module collects feedback information regarding recognized objects for use in the cell selection process. This includes the cell projected area, and the cell centroid position in the image frame. When operated in full automatic mode the system coordinates the control of all software modules, collects available feedback data, and uses both closed- and open-loop control to achieve accurate cell manipulation with minimum operator intervention.

III. SYSTEM AUTOMATION AND CONTROL

The workstation is used to automate the selection, aspiration, manipulation and dispense of single cells. Each cell is dispensed into a microwell; one of the 3 \times 3 microwells forming an array, shown in Fig. 1. The microwells are wet-etched on a fused silica glass wafer using standard photolithography and etching techniques [13]. The microwell array has a pitch of 300 μ m, well diameter of 100 μ m, and well depth of 10 μ m. A flow chart describing the sequence of operations through which cells are aspirated and dispensed is presented in Fig. 5. The system includes two subsystems for: 1) automated single-cell aspiration and 2) automated single-cell dispense. Open-loop control of the X - Y stage vertically aligns the micropipette tip with the center of the petri dish, followed by an “automated single-cell aspiration” process. Once the cell is aspirated, the X - Y stage is translated to vertically align the micropipette tip with the desired microwell (N), followed by the execution of the “automated single-cell dispense” process. In this paper, the number of wells in an array

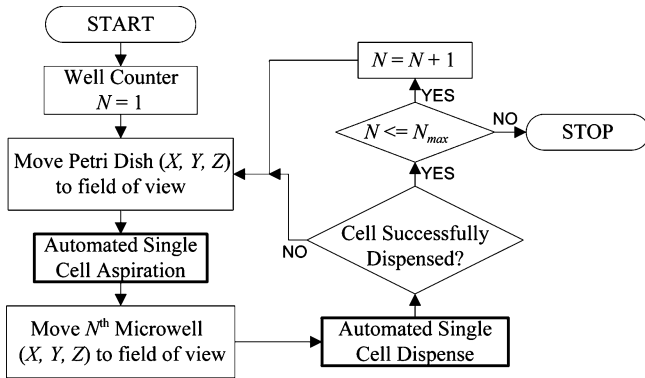


Fig. 5. Flow chart presenting automated cell placement sequence of operations with cell aspiration, and dispensing inner loops.

(N_{max}) is chosen to be nine. Cells are picked up and dispensed one-by-one until each well contains one cell. If a failure to dispense a cell is experienced, the pickup and placement process is repeated.

A. System Setup

System setup for cell manipulation involves multiple manual steps: 1) fluidic circuit cleaning and removal of contaminated media and air bubbles; 2) the vertical alignment of the micropipette orifice with respect to the microscope objective; 3) defining the micropipette tip working plane (p_t) and microscope objective working plane (p_o); and 4) recording the dish center and the well positions.

1) *Fluidic Circuit Cleaning*: Before installing the micropipette assembly to the system, the fluidic circuit must be primed. Priming includes the removal of contaminated media and air bubbles present in the fluid tubing, and filling the fluidic circuit with fresh media. This flushing process is performed by manually controlling the syringe pump, the micropipette valve port (V_p), and the reservoir valve port (V_r). With the valve ports V_p closed and V_r open, the syringe pump is controlled to aspirate filtered fresh media from the reservoir. The valves are then reversed with V_p open and V_r closed and the syringe pump is controlled to push the freshly aspirated media through the circuit, which flushes spent media and air bubbles out of the fluid tubing. This process is repeated until clean media fills all the circuit and only then the micropipette assembly is installed. After installing the micropipette assembly, the flushing process is repeated to ensure that the micropipette is air-free. Flushing, while the micropipette is connected, must be done at small flow rates ($\leq 0.1 \mu\text{L/s}$) to avoid the clogging of the micropipette.

2) *Micropipette Tip Alignment*: The micropipette tip is lowered until it intercepts the focal plane. The X_t and Y_t stages are manually controlled to bring the micropipette orifice to the center of the field of view, aligned with the microscope objective. This procedure is only performed when the pipette is changed or moved.

3) *Working Planes Setup*: Both the culture dish (petri dish) and the microwell array substrate are mounted onto the microscope stage X - Y . An inclination between the working substrate plane (p_s) and the horizontal plane is possible, as shown in

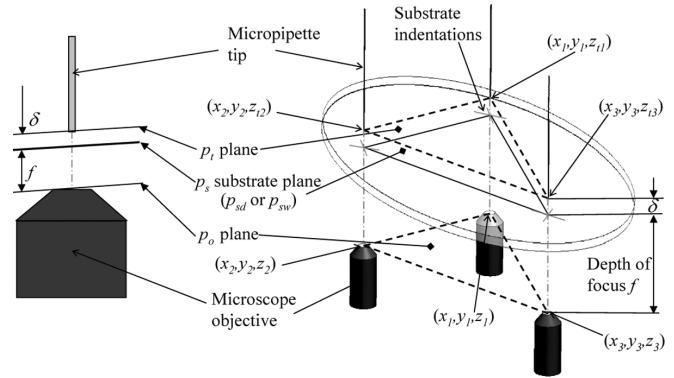


Fig. 6. Planes for system priming showing the substrate plane, p_s , the micropipette plane, p_t , and the microscope object plane, p_o .

Fig. 6. As the stage moves, if the petri dish bottom plane (p_{sd}) is inclined with respect to the horizontal, the following will occur:

- a change in the vertical distance between the micropipette orifice and the dish bottom, δ_d ;
- a change in the vertical distance between the microscope objective and the dish bottom, f_d .

An increase in δ_d may cause the failure to aspirate cells. A decrease in δ_d may cause contact or collision between the micropipette and the dish bottom, damaging the micropipette or contaminating its tip with other cells. In the case of microwell substrate plane (p_{sw}) inclination, the following will be experienced:

- a change in the vertical distance between the micropipette tip and the microwell substrate surface, δ_w ;
- a change in the vertical distance between the microscope objective and the microwell substrate, f_w .

An increase in δ_w may cause failure to properly dispense cells to the desired microwells. A decrease in δ_w may cause a collision between the micropipette tip and the substrate, causing damage to the micropipette. A change in the distance f_d or f_w causes poor image focus. It is therefore necessary to control the Z and Z_t stages to ensure that the distances δ_d , δ_w , f_d , and f_w remain constant. In this work, the value of δ_d is set to $40 \mu\text{m}$, while the value of δ_w is $-10 \mu\text{m}$ (i.e., $10 \mu\text{m}$ deep into the well). The values of f_d and f_w must equal the microscope objective working distance (10.5 mm).

To determine the absolute positions of the stages Z and Z_t for each any X - Y stage position, equations of the planes p_t and p_o are required, see Fig. 6. The planes p_t and p_o are the working planes for the micropipette tip and the microscope objective, respectively, both parallel to the substrate planes p_{sd} and p_{sw} . For every X_i - Y_i microscope stage position, plane p_t includes the micropipette tip position Z_{ti} , while plane p_o includes the microscope objective position Z_i . The equation of the planes p_t and p_o , in the case of the petri dish bottom, are determined with the use of surface features that are easy to focus on. Three surface indentations, inscribed on the petri dish bottom surface, are used. The three indentations, I_1 , I_2 , and I_3 are located at the microscope stage positions (X_1, Y_1) , (X_2, Y_2) , and (X_3, Y_3) . The X - Y stage is translated such that I_1 is in the center of the field of view. The objective Z stage is manually displaced until the indentation I_1 is in focus. This Z stage position is recorded as

Z_1 . The Z_t stage is slowly displaced to lower the micropipette tip until it touches the substrate and is seen to slightly deflect off the surface. This micropipette stage position Z_t is recorded as Z_{t1} . Similarly, (Z_2, Z_{t2}) , (Z_3, Z_{t3}) are recorded for indentations “2” and “3”. The plane equations are determined using the three X - Y stage positions (X_1, Y_1) , (X_2, Y_2) , (X_3, Y_3) , and the recorded (Z_1, Z_2, Z_3) and (Z_{t1}, Z_{t2}, Z_{t3}) . The stage positions Z and Z_t are therefore determined at any X - Y stage position using the plane equations (1) and (2), [15]. An analogous process is carried out for the microwell array; however, the well edges at three of the four microwell array corner wells are used instead of inscribed indentations

$$Z = \frac{1}{c}(d - aX - bY) \quad (1)$$

$$Z_t = \frac{1}{c}(d_t - aX - bY) \quad (2)$$

where

$$a = \begin{vmatrix} 1 & Y_1 & Z_1 \\ 1 & Y_2 & Z_2 \\ 1 & Y_3 & Z_3 \end{vmatrix}, b = \begin{vmatrix} X_1 & 1 & Z_1 \\ X_2 & 1 & Z_2 \\ X_3 & 1 & Z_3 \end{vmatrix},$$

$$c = \begin{vmatrix} X_1 & Y_1 & 1 \\ X_2 & Y_2 & 1 \\ X_3 & Y_3 & 1 \end{vmatrix}, d = \begin{vmatrix} X_1 & Y_1 & Z_1 \\ X_2 & Y_2 & Z_2 \\ X_3 & Y_3 & Z_3 \end{vmatrix},$$

$$d_t = \begin{vmatrix} X_1 & Y_1 & Z_{t1} \\ X_2 & Y_2 & Z_{t2} \\ X_3 & Y_3 & Z_{t3} \end{vmatrix}.$$

4) *Microwells and Dish Position Recording*: The X - Y stage position (X_{wj}, Y_{wj}) for a microwell “ j ” is defined when the micropipette tip position coincides with the center of this well. To calibrate the X - Y positions for all wells in the microwell array, first, the substrate is manually orientated such that the sides of the square bounding the microwell array are orthogonal to the image frame. This is the case when the X -stage position for top-left well (Well-1) is equal to that of the top-right well (Well-3), i.e., $X_{w1} = X_{w3}$. Second, the position for (Well-1) is recorded, (X_{w1}, Y_{w1}) . Knowing the relative well-to-well distance “ l ”, the positions of all the microwells are determined using (3) shown at the bottom of the page.

The centroid of the triangle formed by the three petri dish surface indentation (I_1, I_2, I_3) is defined as the petri dish position (X_{d1}, Y_{d2}) .

B. Automated Single-Cell Aspiration

The automated single-cell aspiration subsystem performs: 1) cell selection; 2) cell positioning with respect to the micropipette tip; and 3) cell aspiration. The aspiration of the cell starts by automatically displacing the micropipette stage to a position Z_{ti} until the micropipette tip-to-dish distance is δ_d ,

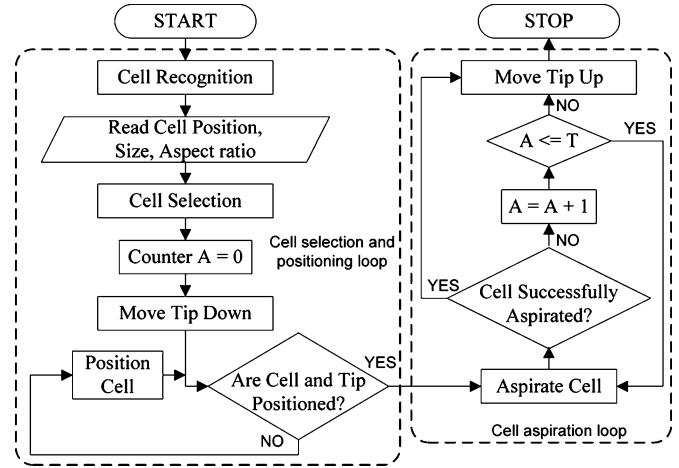


Fig. 7. Flow chart presenting automated cell placement sequence of operations for cell positioning and aspiration.

defined in Section III-A3. The microscope objective is then automatically displaced to a position Z_i until the microscope objective-to-substrate distance is f . A cell is selected and vertically aligned with the micropipette orifice using vision-based feedback. A flow chart describing the sequence of operations in this subsystem is presented in Fig. 7. The flow chart includes two loops, a cell selection and positioning loop, and a cell aspiration loop. In the cell selection and positioning loop, image processing and object recognition techniques are implemented in order to determine the positions of all cells available in the image plane region of interest. This enables determining the relative positions between the micropipette orifice and available cells.

1) *Cell Selection and Positioning*: A common image processing technique called blob analysis is used to detect and analyze distinct two-dimensional shapes within the image field of view. This provides information about the presence or absence, number, location, shape, area, perimeter, and orientation of cells within an image. A set of selection criteria, including cell size, cell position in the field of view, and relative cell-to-cell positions, are used to rank cells of interest. A cell is selected and positioned with the micropipette tip using a closed-loop vision-based feedback controller. The block diagram of this control system is presented in Fig. 8. The X - Y stage hardware has a built-in PID controller that accepts velocity, acceleration, and maximum velocity as parameters. The input to the automated cell-micropipette positioning controller is the micropipette orifice position. The input to the X - Y stage controller is the relative micropipette-cell distance, while the controller output is the actual cell position. The X - Y stage controller aligns the cell with respect to the micropipette orifice by performing an X -displacement, followed by a Y -displacement. This control loop is

$$\begin{bmatrix} X_{w1}, Y_{w1} & X_{w2}, Y_{w2} & X_{w3}, Y_{w3} \\ X_{w4}, Y_{w4} & X_{w5}, Y_{w5} & X_{w6}, Y_{w6} \\ X_{w7}, Y_{w7} & X_{w8}, Y_{w8} & X_{w9}, Y_{w9} \end{bmatrix} = \begin{bmatrix} X_{w1}, Y_{w1} & X_{w1}, Y_{w1} + l & X_{w1}, Y_{w1} + 2l \\ X_{w1} + l, Y_{w1} & X_{w1} + l, Y_{w1} + l & X_{w1} + l, Y_{w1} + 2l \\ X_{w1} + 2l, Y_{w1} & X_{w1} + 2l, Y_{w1} + l & X_{w1} + 2l, Y_{w1} + 2l \end{bmatrix} \quad (3)$$

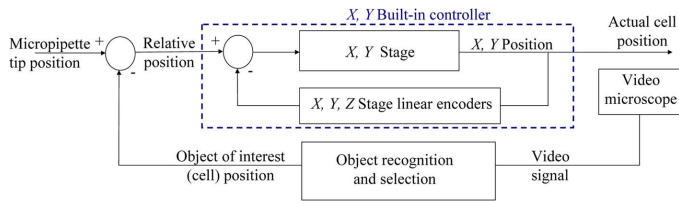


Fig. 8. Block diagram of the automated cell-micropipette positioning control system using vision-based feedback.

repeated until the distance between the micropipette orifice and the cell is less than a specified threshold distance.

2) *Cell Aspiration*: When the selected cell is aligned with the micropipette orifice, aspiration can be performed by applying a negative pressure to the micropipette capillary, which generates a drag force on the cell and pulls it inside. However, strong adhesion forces between cells and the culture dish bottom, due to surface protein interaction with the dish surface, generate an opposing force and cause some difficulties in the aspiration. To overcome these adhesion forces, we conceived and implemented a method comprising the application of a positive pressure pulse strong enough to displace the cell from an adhered state to a suspended state. The now non-adherent (suspended) cell is identified and an attempt is made to aspirate this cell into the capillary tip using negative pressure pulses, each aspirates a volume of medium (V_{pulse}). A negative pressure pulse causes the cell to move towards the micropipette orifice. This process, visually monitored, is repeated as required until the cell is successfully aspirated and disappears into the micropipette. The maximum number of attempts is set at (T). If the desired cell is not successfully aspirated, a new cell is selected, as seen in the cell aspiration loop of Fig. 7. The location of the cell inside the micropipette depends upon the magnitude of the volume V_{pulse} .

C. Automated Single-Cell Dispense

The automated single-cell dispense subsystem is responsible for the placement of an aspirated cell into the desired microwell. The microscope stage (X - Y) is first open-loop controlled to vertically align the desired microwell with the micropipette orifice. Knowing the stage position of the microwell (X_{wi} , Y_{wi}), the objective stage (Z) is automatically displaced to the position Z_{wi} , calculated using (1), where the objective-to-substrate distance is f . A flow chart of the sequence of operations in the automated cell dispense subsystem is presented in Fig. 9. Cell dispense is then performed through the following fully automated steps:

- 1) the micropipette is vertically lowered to the position Z_{twi} , calculated using (2), where the tip-to-substrate distance is δ_w ;
- 2) a positive pressure is applied to the micropipette capillary, generating an ejection force on the cell;
- 3) the micropipette is displaced upwards;
- 4) vision-based feedback, resulting from image processing and blob analysis, indicates the presence or the absence of a cell in the microwell.

These four steps are repeated until either the cell is successfully dispensed or the maximum number of dispense attempts (S) is reached. The fluidic dispense of the cells must be slow and gentle so as to not cause damage to the cell.

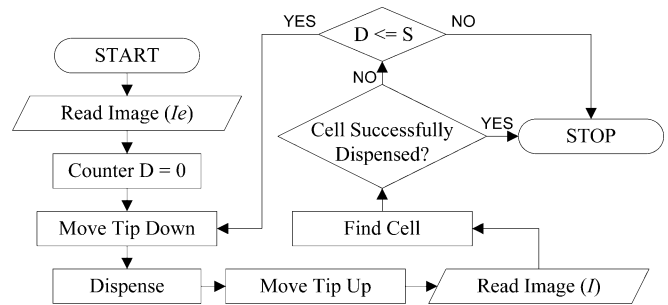


Fig. 9. Flow chart presenting automated cell placement sequence of operations for cell dispensing.

IV. RESULTS AND DISCUSSION

This section describes the experiments conducted to evaluate the performance of the automated single-cell loading system. Using vision-based feedback, the target cell is selected based on predefined selection criteria. The target cell is aspirated in the manner presented in Section III-B2. The aspirated cell is dispensed into the microwell as described in Section III-C. Image processing and object recognition techniques, including background subtraction and morphological closing, are used to inspect the presence of the cell in the well. A discussion of the results concludes this section.

A. Cell-Line Information

Three immortalized human cell lines are of interest to the Microscale Life Sciences Center (MLSC) [9] and were used in this work: 1) A549 human alveolar basal epithelial cell carcinoma; 2) K562 myelogenous leukemia; and 3) Barrett's esophagus (BE). The cell lines are all adherent cells cultured in cell culture flasks. Single cells must first be released from the cell culture flask and brought into a suspended state. Cell cultures with no less than 90% confluence are used. To release the cells, the adherent culture is rinsed with Phosphate-Buffered Saline (PBS), then trypsinized. Traces of trypsin are removed by the addition of 10% serum DMEM medium. The suspension is transferred to a 15 mL tube, where centrifugation and supernatant removal are performed. Cell preparation is completed by the addition of Ham's F-12 medium with 10% serum. The target density of cells in the petri dish is approximately 20 cells/ μL . A higher cell concentration may lead to the aspiration of multiple cells, which is undesirable. BE cells were selected for most of our cell manipulation experiments. The diameters of these suspended cells were measured and the average suspended cell diameter was found to be 15 μm . Manipulation of live cells requires special precautions and conditions, including a contamination free environment, regulated operating temperature, media composition, 5% CO_2 and pH. Since this paper presents only results intended to demonstrate preliminary system performance, experiments were performed at ambient conditions.

B. Cell Selection and Aspiration

The CCD camera captures 5 megapixel color (RGB) images (2560×1920 pixels) of the petri dish bottom with cells suspended in medium, as presented in the example in Fig. 10(a). The images are processed to recognize all cells available in the image frame. Background subtraction is the first in a series of

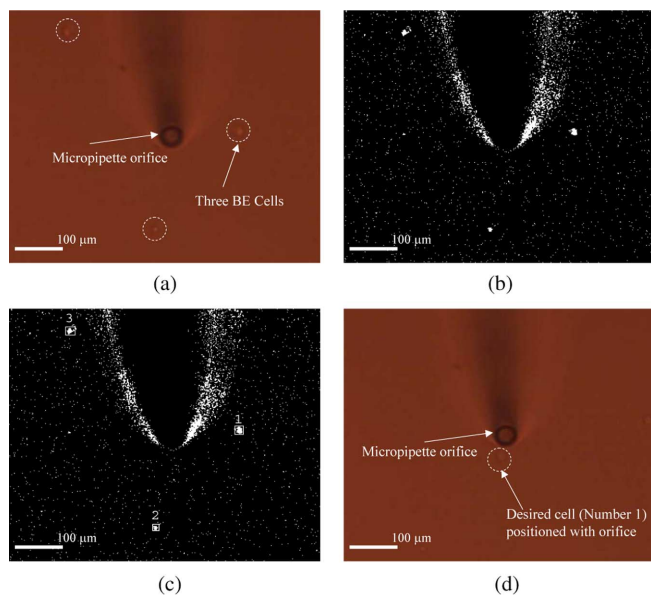


Fig. 10. Steps describing the automated selection and positioning of a single live cell in a culture dish. (a) Bright field image of tip and three BE cells. (b) Thresholding, image subtraction and processing. (c) Cells recognition. (d) Positioning cell at tip orifice.

image processing steps applied to each image. Thresholds are applied to the image resulting in a binary image showing available cells and other particles or defects that are identified as lesser objects [see Fig. 10(b)]. The final processing step is the classification of live cells to differentiate them from other objects, debris and defects. Cell classification includes two steps:

- only objects having areas close to that of cells are selected, falling within defined maximum and minimum values;
- the object height-to-width (aspect) ratio must fall in the range of 0.8 and 1.3 to eliminate elongated objects.

Fig. 10(c) shows three cells that were correctly classified in the image frame based on these criteria. Each cell centroid is determined in image coordinates, in units of pixels. The micropipette orifice is positioned in the center of the image frame during initial system setup. With the micropipette orifice and cell positions known, the x and y relative positions (in pixels) between the cells and the micropipette orifice are determined. Measurements in pixels are converted to the global coordinates using coordinate transformation operations. An additional constraint that must be satisfied for cell selection is that the relative distance between any two cells must be larger than a chosen value of $60 \mu\text{m}$, or both cells are excluded. This reduces the chance of multiple cell aspiration. For cells satisfying all conditions, the cell closest to the micropipette tip is selected. Therefore, cell-1 in Fig. 10(c) was selected by the automated system. To align the cell with the micropipette orifice, closed-loop control is used to displace the X - Y horizontal stage in the x - and then the y -directions, as indicated in the block diagram of Fig. 8. Fig. 10(d) shows the cell number “1” positioned at the orifice of the micropipette. Once automated positioning is performed, the cell aspiration loop in Fig. 7 is activated. The applied flow pulses have a volume $V_{\text{pulse}} = 2 \text{ nL}$ at a flow rate of 200 nL/s . This is followed by an open-loop control of the X -, Y -, Z -, and Z_t -stages to position the micropipette orifice with respect to an array microwell of known coordinates.

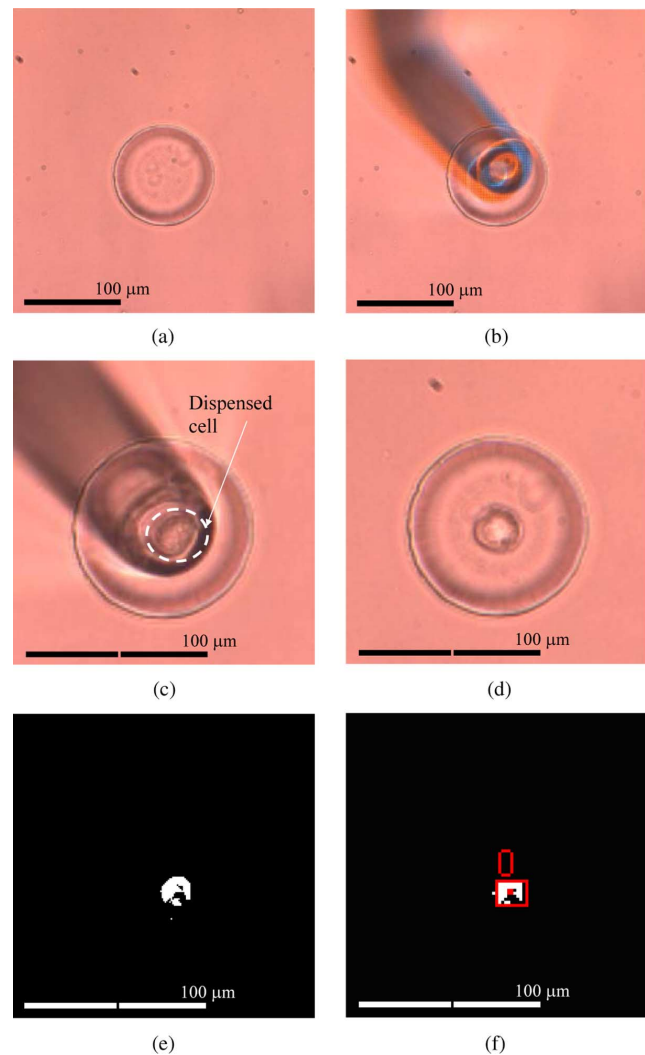


Fig. 11. Steps describing the automated dispense of a single cell into a microwell. (a) Empty microwell where cell is to be dispensed. (b) Micropipette orifice is lowered into empty microwell. (c) Cell is dispensed. (d) Micropipette is displaced upwards. (e) Image processing to inspect the presence of a cell. (f) A single cell is detected.

C. Cell Dispense

Single cells are automatically dispensed in the desired microwells in the manner described in the flow chart in Fig. 9. Difficulties are faced when identifying the nearly-transparent cells in their background and surroundings, and in differentiating between cells and artifacts such as chips or debris on the substrate surface. A computer vision object recognition method was implemented to solve these problems: An image of the empty microwell is captured before lowering the micropipette [Fig. 11(a)]. Once the empty well image is captured, the tip is lowered [Fig. 11(b)], a cell dispense attempt is performed [Fig. 11(c)], and the micropipette is withdrawn upwards. The presence of a dispensed cell in the microwell is verified by subtracting the recorded image of the empty microwell [Fig. 11(a)] from the post-dispense images of the object well (Fig. 11(d)). The difference image is segmented by applying a threshold, resulting in a binary image [Fig. 11(e)]. Morphological closing is performed to remove minor particles, followed by the blob analysis process to detect the presence of a cell in the well. The blob

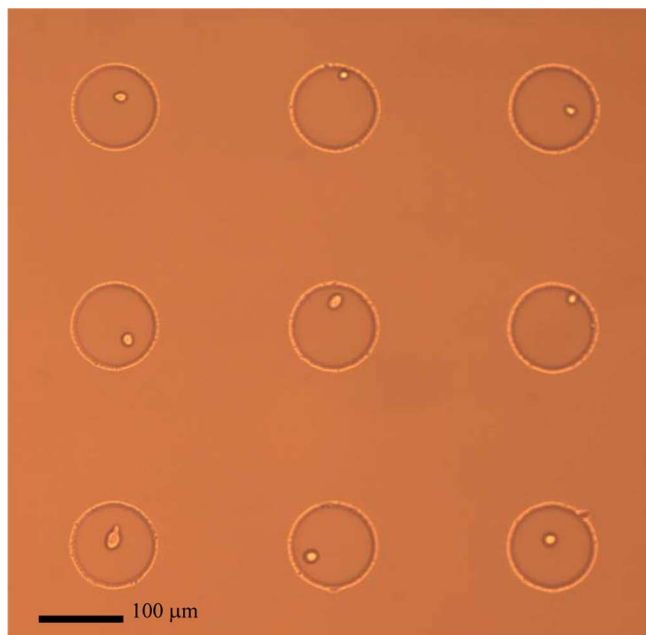


Fig. 12. A 3×3 microwell array where each microwell is loaded with one cell.

analysis is performed using the IMAQ Vision software (National Instruments). Fig. 11 shows a successful single-cell dispense. The microwell image was processed and a single cell was recognized, indicating the dispense of the cell, see Fig. 11(f). In our current applications, positioning the cell at any location inside the well fully satisfies our performance specifications.

D. Discussion

Experiments were conducted to evaluate the performance of the cell dispense system. The system was optimized for cell selection and placement accuracy. Optimization for speed was not addressed, where all motorized stages operations were performed at intermediate speeds. Cells available in the field of view were visually inspected and manually selected based on their size, state (adherent or suspended), and viability. A cell was selected by placing a crosshair at its center using the software GUI. Closed loop positioning presents the cell to the orifice of the micropipette. This is followed by the aspiration of the positioned cell.

Iterations were run to load single cells into 163 wells. Of the 163 loading attempts, 151 cells (92.60%) were successfully loaded into microwells, while 12 failed. For the 12 failures, 11 cells were successfully loaded on the second attempt, while one was loaded on the third attempt.

In summary, the total number of loading attempts was 176, of which 163 were successful. Therefore, the probability of successfully loading a single cell was 93.1%. Using the closed-loop control algorithm, all 163 wells were loaded with a 100% loading rate. The average time needed to successfully load one cell, between cell selection and dispense, was 40 s. Fig. 12 shows a 3×3 microwell array, loaded with cells. Cell loading failures were attributed to one of the following:

- escape of the cell from the micropipette orifice when vertically withdrawing the tip out of the culture dish solution, or

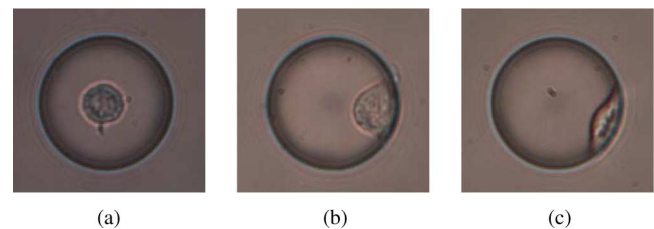


Fig. 13. Effect of the incubation time on a single cell stretching and adhesion to the substrate: indicating cell viability. (a) Before incubation, (b) 30 minutes, and (c) 2 hours.

when vertically immersing the tip into the microwell array solution;

- a cell is dispensed in well, but when the micropipette tip retracts, the generated fluid disturbance pulls the cell out of the well.

To investigate the viability of loaded cells, Barrett's esophagus (BE) cells loaded to wells were incubated over a period of 2 h and inspected every 30 min. Loaded cells were found to adhere to the substrate, tending to stretch, and crawling towards the wall of the well. These are signs of cell viability [17], indicating the gentleness of the process. Fig. 13 presents a example of a cell, loaded into a $50 \mu\text{m}$ well before incubation, after 30 min, and 2 h of incubation, respectively.

V. CONCLUSION

This paper presents the engineering testbed phase of the development of an automated workstation for single-cell manipulation. Hardware components, software, control and automation methodology and experimental results are presented. The system incorporated the commonly used approach of aspirating cells using glass capillary micropipettes, while adding subsystems that enable full automation of this process.

The uniqueness of this proposed system, compared to other systems, is in its ability to transfer individual cells from a culture dish to their target locations at a 100% success rate. Vision-based feedback was used to control the cell selection and capture, in addition to check the cell dispense. Experimental results indicate that a high success rate is feasible using the proposed cell transfer method. The time required to transfer a single cell can be significantly reduced, by operating the microscope and the micropipette stages at their maximum speeds.

VI. FUTURE WORK

Future work includes incorporating a fluidic manipulator that is capable of manipulating small volumes of fluid (in the picoliter range) with high flow rate control capability. This enables knowledge of the exact location of an aspirated cell within the micropipette, reducing the chance of cell loss, and therefore improving success rates. The use of a picoliter fluidic manipulator will also enable the aspiration and the stacking of multiple cells in the micropipette, where they can be dispensed, one-by-one, into microwells (stacked-single-cell loading). This will significantly increase the throughput and reduce the time needed to load a single-cell into a well. Operating the motorized stages at their maximum speeds, in addition to stacked-single-cell loading, is expected to reduce cell transfer by 75% or more.

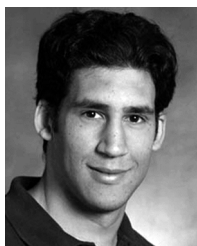
A significant increase in throughput is expected with reduced time needed to load single cells into a wells.

ACKNOWLEDGMENT

The authors gratefully acknowledge the following for their assistance: A. Mohammadreza, A. Lécluse, Dr. R. Johnson, Dr. Y. Li, Dr. H. Zhu, J. Houkal, Dr. L. Kelbaskas, V. Nandakumar, C. Hemphill, and J. Grover.

REFERENCES

- [1] K. K. Sanford, W. R. Earle, and G. D. Likely, "The growth in vitro of single isolated tissue cells," *J. Nat. Cancer Inst.*, vol. 9, pp. 229–246, 1948.
- [2] R. M. Hochmuth, "Micropipette aspiration of living cells," *J. Biomechanics*, vol. 33, pp. 15–22, 2000.
- [3] J. Y. Shao and R. M. Hochmuth, "Micropipette suction for measuring piconewton forces of adhesion and tether formation from neutrophil membranes," *Biophysical J.*, vol. 71, pp. 2892–2901, 1996.
- [4] K. Wewetzer and B. Seilheimer, "Establishment of a single-step hybridoma cloning protocol using an automated cell transfer system: Comparison with limiting dilution," *J. Immunological Methods*, vol. 179, pp. 71–76, 1995.
- [5] A. Ashkin, J. M. Dziedzic, and T. Yamane, "Optical trapping and manipulation of single cells using infrared laser beams," *Nature*, vol. 330, pp. 769–771, 1987.
- [6] K. Svoboda and S. M. Block, "Biological applications of optical forces," *Annu. Rev. Biophys. Biomolecular Structure*, vol. 23, pp. 247–285, 1994.
- [7] D. G. Grier, "A revolution in optical manipulation," *Nature*, vol. 424, pp. 810–816, 2003.
- [8] J. Voldman, "Electrical forces for microscale cell manipulation," *Annu. Rev. Biomed. Eng.*, vol. 8, pp. 425–454, 2006.
- [9] The Microscale Life Sciences Center. [Online]. Available: <http://www.life-on-a-chip.org>
- [10] M. E. Lidstrom and D. R. Meldrum, "Life-on-a-chip," *Nature Rev. Microbiol.*, vol. 1, pp. 158–164, Nov. 2003.
- [11] T. W. Molter, M. R. Holl, J. M. Dragavon, S. C. McQuaide, J. B. Anderson, A. C. Young, L. W. Burgess, M. E. Lidstrom, and D. R. Meldrum, "A new approach for measuring single cell oxygen consumption rates," *IEEE Trans. Autom. Sci. Eng.*, vol. 5, pp. 32–42, Jan. 2008.
- [12] T. W. Molter, S. C. McQuaide, M. T. Suchorolski, T. J. Strovas, L. W. Burgess, D. R. Meldrum, and M. E. Lidstrom, "A microwell array device capable of measuring single-cell oxygen consumption rates," *Sens. Actuators: B. Chemical*, vol. 135, pp. 678–686, 2009.
- [13] H. Zhu, M. Holl, T. Ray, S. Bhushan, and D. R. Meldrum, "Characterization of deep wet etching of fused silica glass for single cell and optical sensor deposition," *J. Micromech. Microeng.*, vol. 19, no. 065013, 2009.
- [14] Y. H. Anis, M. R. Holl, and D. R. Meldrum, "Automated vision-based selection and placement of single cells in microwell array formats," in *Proc. Int. Conf. Autom. Sci. Eng.*, 2008, pp. 315–320.
- [15] W. Gellert and C. Van Nostrand Reinhold, *The VNR Concise Encyclopedia of Mathematics*. New York: Van Nostrand Reinhold, 1989.
- [16] ATCC The Global Bioresource Center. [Online]. Available: <http://www.atcc.org>
- [17] B. M. Gumbiner, "Cell adhesion: The molecular basis of tissue architecture and morphogenesis," *Cell*, vol. 84, pp. 345–358, 1996.



Yasser H. Anis (M'05) was born in Giza, Egypt. He received the B.S. and M.S. degrees in mechanical engineering from Cairo University, Giza, Egypt, in 2001 and 2004, respectively, and the Ph.D. degree in mechanical engineering from the University of Toronto, ON, Canada, in 2007.

Since 2007, he has been with the Center for Ecogenomics, Biodesign Institute, Arizona State University as a Postdoctoral Research Associate and now as an Assistant Research Scientist. He is affiliated with the Department of Mechanical Design and Production at Cairo University, Egypt. His current research interests include automation, robotics, control, and microelectromechanical systems.

Dr. Anis is member of the Institute of Electrical and Electronics Engineers (IEEE), the American Society of Mechanical Engineers (ASME), the International Society for Optical Engineers (SPIE), and the Egyptian Syndicate of Engineers.



Mark R. Holl (M'01) was born in Champaign, IL. He received the B.S. degree in mechanical engineering from Washington State University, Pullman, in 1986, and the M.S. and Ph.D. degrees in mechanical engineering from the University of Washington, Seattle, in 1990 and 1995.

From 1987 to 1989, he worked at Boeing Commercial Aircraft in Manufacturing, Research, and Development. From 1995 to 2000, he worked with Prof. P. Yager in Bioengineering at the University of Washington to assist in the development and commercialization of micro total analysis system technologies. He was a principal inventor with Dr. P. Yager of a laminate-based microfluidic technology and a founding member of a startup company, Micronics, Inc. From 2000 to 2006, he collaborated with Prof. D. Meldrum at the University of Washington in developing microfluidic technologies for biomedical and genome science applications, first as a Research Engineer (2000) and subsequently as a Research Assistant Professor (2001–2006). In 2007, he moved to the Center for Ecogenomics in the Biodesign Institute, Arizona State University, as a Research Scientist. Currently, he maintains his affiliation with the Center for Ecogenomics, is an Investigator with the Microscale Life Sciences Center (an NIH Center of Excellence in Genomic Sciences), and is the Associate Director of Development for the Biodesign Institute Impact Accelerator. His research interests include systems integration for total analysis systems, microscale systems for biological applications, bioprocess automation, sensor development, and process characterization and control with emphasis on biomedical, genomic, and proteomic science applications.

Dr. Holl is a member of the American Association for the Advancement of Science (AAAS), ASME, and the International Society for Optical Engineers (SPIE).



Deirdre R. Meldrum (M'93–SM'00–F'04) received the B.S. degree in civil engineering from the University of Washington, Seattle, in 1983, the M.S. degree in electrical engineering from the Rensselaer Polytechnic Institute, Troy, NY, in 1985, and the Ph.D. degree in electrical engineering from Stanford University, Stanford, CA, in 1993. She is a graduate of the Stanford Executive Program 2009.

As an Engineering Co-op Student at the NASA Johnson Space Center in 1980 and 1981, she was an Instructor for the astronauts on the Shuttle Mission Simulator. From 1985 to 1987, she was a member of the Technical Staff at the Jet Propulsion Laboratory working on the Galileo spacecraft, large flexible space structures, and robotics. From 1992 to 2006, she was a Professor of Electrical Engineering and Director of the Genomation Laboratory, University of Washington. Currently, she is Dean of the Ira A. Fulton School of Engineering, Professor of Electrical Engineering, and Director of the Center for Ecogenomics, Biodesign Institute, Arizona State University. Her research interests include genome automation, microscale systems for biological applications, ecogenomics, robotics, and control systems.

Dr. Meldrum is a member of the American Association for the Advancement of Science (AAAS), ACS, AWIS, HUGO, Sigma Xi, and SWE. Her honors include a NIH Special Emphasis Research Career Award (SERCA) in 1993, a Presidential Early Career Award for Scientists and Engineers in 1996 for advancing DNA sequencing technology, Fellow of AAAS in 2003, Distinguished Lecturer for IEEE Robotics and Automation Society 2006–2009, Best Paper of the Year 2006 in the IEEE TRANSACTIONS ON AUTOMATION SCIENCE AND ENGINEERING, Director of an NIH Center of Excellence in Genomic Sciences called the Microscale Life Sciences Center from 2001 to 2011, and Senior Editor for the IEEE TRANSACTIONS ON AUTOMATION SCIENCE AND ENGINEERING from 2003–present.